Available online at www.sciencedirect.com
SCIENCE DIRECT®
Journal of Theoretical Biology 236 (2005) 276–290
Journal of Theoretical Biology
www.elsevier.com/locate/yjtbi

A model for seasonal phytoplankton blooms

Amit Huppert[a,*], Bernd Blasius[a,b], Ronen Olinky[a], Lewi Stone[a]

[a]Department of Zoology and the Porter Super Center for Ecological and Environmental Studies, Tel Aviv University, Ramat-Aviv, Tel Aviv 69978, Israel
[b]Department of Physics, University of Potsdam, Am Neuen Palais 10, D-14415 Potsdam, Germany

Received 10 November 2004; received in revised form 8 March 2005; accepted 8 March 2005
Available online 23 May 2005

Abstract

We analyse a generic bottom-up nutrient phytoplankton model to help understand the dynamics of seasonally recurring algae blooms. The deterministic model displays a wide spectrum of dynamical behaviours, from simple cyclical blooms which trigger annually, to irregular chaotic blooms in which both the time between outbreaks and their magnitudes are erratic. Unusually, despite the persistent seasonal forcing, it is extremely difficult to generate blooms that are both annually recurring and also chaotic or irregular (i.e. in amplitude) even though this characterizes many real time-series. Instead the model has a tendency to 'skip' with outbreaks often being suppressed from 1 year to the next. This behaviour is studied in detail and we develop analytical expressions to describe the model's flow in phase space, yielding insights into the mechanism of the bloom recurrence. We also discuss how modifications to the equations through the inclusion of appropriate functional forms can generate more realistic dynamics.

Keywords: Phytoplankton; Bloom; Model; HAB; Seasonal forcing; Nutrients

1. Introduction

Aquatic ecologists have long been fascinated by the non-equilibrium dynamics of explosive phytoplankton blooms. Often such blooms are viewed as a signal of impending eutrophication, indicating that ecosystem balance is lost and that nutrients may have reached unacceptably high levels, at least high enough to support massive bloom formations. Sometimes, however, annual phytoplankton blooms are more of a natural ecosystem event than a cause for concern or danger to water quality. In such circumstances, periodic algae blooms are better viewed as an evolutionary successional development of phytoplankton species that characterizes their lifecycle and response to surrounding ecological and environmental conditions. As some phytoplankton species are toxic, their appearance in large numbers has obvious dangerous implications. Collectively referred to as Harmful Algae Blooms (HAB's), these events have the potential to damage or kill higher organisms such as zooplankton, shellfish, and fish as their toxins mobilize up through the foodchain, sometimes leading to human poisoning via ingestion of contaminated food sources. HAB's have enormous economic implications in terms of public health, commercial fisheries and even tourism (Anderson et al., 2000). Algae blooms are also responsible for the spread of some epidemics. In Bangladesh, for example, cholera outbreaks appear to originate from annual bloom events in the Bay of Bengal (Colwell, 1996). Given the importance of these many different and distinctive types of phytoplankton blooms, our goal is to develop modelling approaches for understanding their underlying dynamics.

Many aquatic systems endure harsh seasonal changes, as for example the changing physical stratification in lakes and oceans, which have large impact on ecosystem dynamics and often control bloom dynamics. Our goal is to model the complex dynamics of seasonally recurring algae blooms in a manner that realistically

*Corresponding author.
E-mail addresses: ahuppert@whoi.edu (A. Huppert), lew521@yahoo.com (L. Stone).

0022-5193/$ - see front matter © 2005 Elsevier Ltd. All rights reserved.
doi:10.1016/j.jtbi.2005.03.012

matches ecological data sets. In this respect, we do not focus on single transient algae blooms which have already been the subject of an extensive modelling analysis in earlier papers (Huppert et al., 2002, 2004). Fig. 1 displays time-series of different algal species from different locations in lakes and oceans around the world, for example, in Lake Kinneret (Fig. 1a), the German Bight (Fig. 1b) and San Francisco Bay (Fig. 1c). All time-series show recurring bloom events which are triggered at roughly the same time each year (usually Spring). Each bloom is characterized by a period of rapid algae growth followed by a crash in population numbers, after which there is a long quiescent period where phytoplankton numbers remain minimal. Our model will be used to describe and explain some of the features seen in such time-series.

There are many factors which affect the initiation and rapid multiplication of algal numbers. In this paper, we focus on phytoplankton blooms that are mainly controlled by nutrients rather than by higher tropic levels (O'Brien, 1974; Ebenhoh, 1988; Evans, 1988; DeAngelis, 1992; Stone and Berman, 1993; Franke et al., 1999). Bottom-up control is important in many cases. For example, there are many zooplankton species that tend not to graze toxic red tide algae. Similarly, other types of algae have spines, cellulose cell walls and/or are large in size which protects the phytoplankton from being grazed. The large *Peridinium gatunense* diatom bloom in Lake Kinneret, for example, is rarely if ever grazed by zooplankton. In such cases "top-down" models are inadequate as a general description of phytoplankton blooms. Yet most models to date rarely use the required bottom-up formulation for these systems. To help fill this gap, Huppert et al. (2002) studied the simplest nutrient–phytoplankton (NP) model that succeeds in modelling algae blooms based on a 'bottom-up' approach. However, the generic NP-model is unable to generate periodic cycles (see Appendix A), and is thus unsuitable for modelling outbreaks that recur seasonally. We extend the basic NP-model by introducing periodic seasonal forcing which induces all kinds of complex dynamics from limit-cycles to chaos. This is in contrast to several studies of a particular class of NP models (the classic Droop model), which fails to generate complex dynamics (Pascual, 1994; Smith, 1997). Note, however, that it has recently been theoretically demonstrated that chaotic dynamics are possible in externally driven chemostats with additional phytoplankton mortalilty (Blasius and Clodong, 2004).

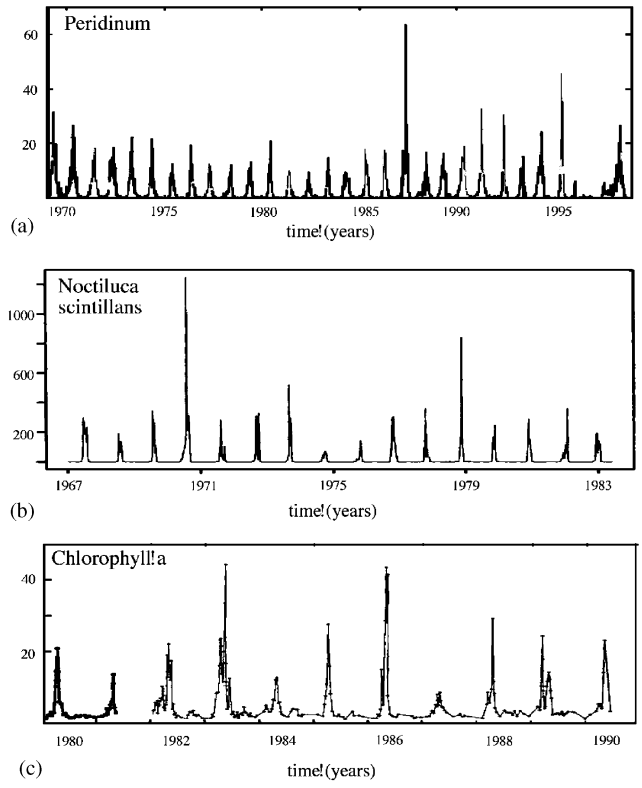

Fig. 1. Time-series of phytoplankton from different lakes and oceans around the world. (a) Annual *Peridinium gatunense* blooms in Lake Kinneret, Israel (given in units of mg/m^3). Data courtesy of Utza Pollingher and Tamar Zohary. (b) Annual *Noctiluca scintillans* blooms in the German Bight. Adapted from Beltrami and Carroll (1994) (given in units of cells/litre); data originated from Dr. G. Uhlig of the Biological Research Station, Helgoland, Germany. (c) Annual blooms in South San Francisco Bay, USA (chlorophyll *a* concentration in units of mg/m^3). Adapted from Cloern (1991).

Previously we have studied populations whose abundances are highly erratic or chaotic but their period length is remarkably constant—a behaviour we referred to as UPCA (Uniform Phase evolution with Chaotic Amplitudes; see Blasius et al., 1999). A glance at the phytoplankton time-series of Fig. 1 shows that UPCA might be an appropriate description for many recurring algae blooms. (Another possibility is that the variability may be explained by the addition of stochasticity, something which we explore elsewhere (Barnea, Solow, Stone manuscript).) However, most conventional ecological models are unable to reproduce this behaviour. Recently, we developed a 3 species food web model which has the above characteristics (Blasius et al., 1999), but the possibility of finding UPCA in forced models has so far been neglected. Our own extensive simulation studies have revealed that it is surprisingly difficult to generate UPCA dynamics in forced NP models. In the present paper we discuss what is to our knowledge, the first two level seasonally forced model that is able to generate UPCA dynamics.

2. A simple nutrient–phytoplankton model

The forced NP compartment model consists of two variables, nutrients levels N, and phytoplankton biomass P, connected through the following system of

equations (Huppert et al., 2002):

$$\dot{N} = a - b\beta(t)NP - eN,$$

$$\dot{P} = c\beta(t)NP - dP. \quad (1)$$

The model has initial conditions $N(0) = N_0 > 0$ and $P(0) = P_0 > 0$. It is assumed that there is an external source of nutrients flowing into the system at a constant rate a. The Lotka–Volterra interaction term, NP, is used for modelling the phytoplankton uptake of nutrients, and implies that the probability of a phytoplankton utilizing a nutrient is proportional to the product of their relative abundances. The final uptake rate is determined by the parameters b and c. In addition, phytoplankton is removed from the water column through mortality as determined by the parameter d. This parameter also takes into account relatively constant grazing or predation by higher tropic levels such as zooplankton and fish. Finally, there is a small nutrient loss parameter e which represents sinking of nutrients from the epilimnion down to the hypolimnion and therefore making these nutrients unavailable for phytoplankton uptake (DeAngelis, 1992).

Seasonal environmental conditions such as water temperature, salinity, light and thermocline depth are often important to different degrees depending on the system under investigation. In the above model, we suppose that there is a seasonal modulation of phytoplankton growth so that some periods of the year have environmental conditions more suitable for growth than others. The modulation of phytoplankton growth β can be represented as a periodic function $\beta(t) = \beta(t + \tau)$ with maxima at the optimal season (e.g. spring for many phytoplankton blooms). Here, τ is the period of forcing, which in this work is taken to be annual. A convenient and commonly applied scheme is that of sinusoidal forcing

$$\beta(t) = 1 - \delta \sin(\omega t). \quad (2)$$

When the forcing is annual, and t is in units of years, then $\omega = 2\pi$. The parameter δ $(0 < \delta < 1)$ controls the strength of the forcing. Obviously if $\delta = 0$, the model collapses to an unforced system. Although Eq. (2) is a crude simplification, it serves as a first approximation for investigating how seasonal factors influence the model's dynamics. For some biological applications seasonal changes might be better approximated by a step-function. This is true in some lakes (e.g. Lake Kinneret) where the seasonal climate dynamics and stratification patterns are more reasonably approximated by a step-function consisting of a 'high season' where conditions are optimal for growth, and a 'low season' where growth is suppressed. Mathematically this forcing could be represented as

$$\beta(t) = \begin{cases} \beta^+ = 1 + \delta, & \text{High season,} \\ \beta^- = 1 - \delta, & \text{Low season,} \end{cases} \quad (3)$$

where again δ $(0 < \delta < 1)$ controls the strength of the seasonal forcing. Here β takes only two values, one that is high (β^+) and the other low (β^-). The time-scale is such that there are two equally long seasons per time period $\tau = 2\pi/\omega$. Thus for annual forcing $\tau = 1$ and $\omega = 2\pi$.

We have found the dynamics produced by the NP model (Eq. (1)) are very robust to a wide array of periodic functions in that most of the model's range of dynamics can be reproduced independent of the qualitative form of the forcing (i.e. assuming forcing frequency and mean amplitude remain unchanged). Both sinusoidal and step-function forcings are examined in this paper, although we take advantage of the step-function forcing for analytical calculations. For convenience only, from here on our notation is based on the step-function formulation for β (Eq. (3)).

The model can be simplified if it is written in dimensionless variables

$$N' = \frac{c}{d}N, \quad P' = \frac{b}{d}P, \quad t' = dt,$$

$$I = \frac{ac}{d^2}, \quad q = \frac{e}{d}, \quad \omega' = \frac{\omega}{d} = \frac{2\pi}{d}. \quad (4)$$

Dropping the dashes the model becomes

$$\dot{N} = I - \beta^{\pm}NP - qN,$$

$$\dot{P} = \beta^{\pm}NP - P, \quad (5)$$

where $\beta^{\pm}$ is given by Eq. (3). Nutrient uptake b and c and the plankton loss rate d have effectively been scaled out, leaving only the scaled nutrient inflow/outflow parameters I and q. Thus, the forced model depends on only four parameters I, q, ω and δ.

3. Analysis of the model

3.1. The 'generic' bloom event

An understanding of the mechanisms that lead to a single bloom event is a prerequisite for embarking on an analysis of the forced NP model, and we therefore first review basic concepts (see Huppert et al., 2002 for full details). In the case of small nutrient loss compared to inflow, $2q < I$, the unforced model (Eq. (5), $\delta = 0$) has a globally stable equilibrium given by

$$P^* = I - q, \quad N^* = 1. \quad (6)$$

A plot of the bloom's evolution in the time-domain may be seen in Fig. 2a, and it can be divided into three stages:

- *stage* i: linear nutrient (N) build up;
- *stage* ii: phytoplankton bloom (rapid rise in P) and subsequent depletion in nutrients (N);
- *stage* iii: bloom crash (rapid decline in P).

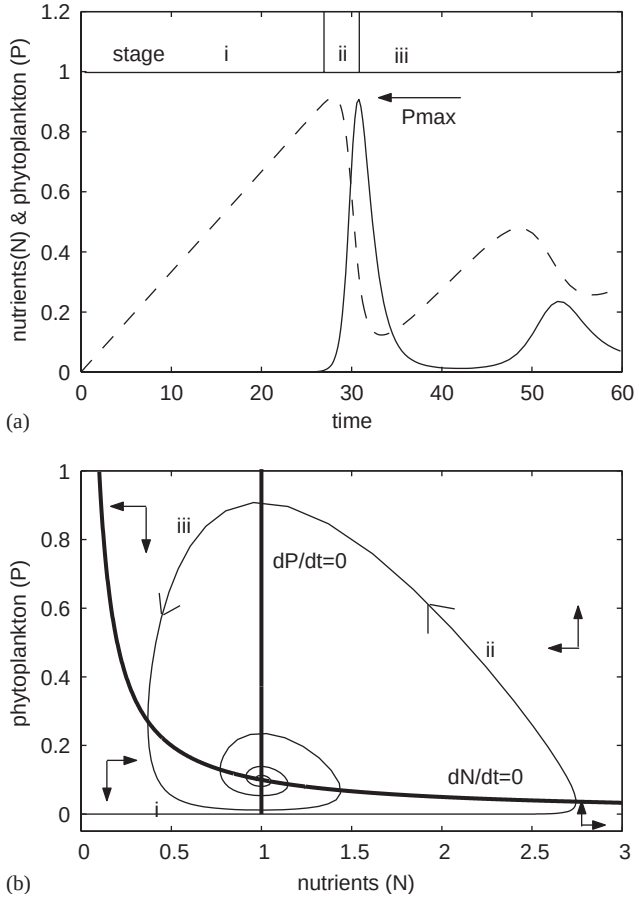

Fig. 2. (a) Time-series plot of Eq. (5) with phytoplankton (P) (solid line), limiting nutrient (N) (dotted line). Nutrients slowly build up linearly until initiation of the bloom. Parameters are: $I = 0.075$, $q = 0$, with initial conditions $P_0 = 0.05$, $N_0 = 0.0005$. For the purposes of illustration, nutrient levels were rescaled and reduced by a factor of three. (b) Phase-plane diagram of the phytoplankton bloom. The arrows indicate the direction (always counterclockwise) that the trajectory 'flows' in the phase plane. The different stages- i, ii, and iii are indicated at the top of the graph. The nullclines are conceptually important for understanding how the trajectory flows in the phase plane. The N-nullcline ($\frac{dN}{dt} = 0$) divides the phase plane in two with all points above the nullcline characterized by $\frac{dN}{dt} > 0$ and all points below having $\frac{dN}{dt} < 0$. Similarly the P-nullcline ($\frac{dP}{dt} = 0$) divides the phase plane in two with all points to the left of the nullcline characterized by $\frac{dP}{dt} < 0$ and all points to the right having $\frac{dP}{dt} > 0$. As such, the direction of flow in the phase plane is defined by the coordinates of the trajectory and its location relative to the two nullclines.

A typical simulation run begins with initial conditions (N_0, P_0) in the lower left region of the phase plane (Fig. 2b; see figure legend for explanation of phase-plane dynamics). The trajectory rotates anticlockwise in phase space as it spirals to equilibrium passing in turn through each of the three stages. Because the initial conditions (N_0, P_0) are in the lower left region of the phase plane, at first $\dot{P} < 0$ and $\dot{N} > 0$; although not visible in this figure the phytoplankton levels initially decline and there is a slow constant nutrient build up due to the inflow I (*stage*-i). The nutrient levels N continue to build up until they reach the P-nullcline at which point the algae bloom is triggered (*stage*-ii). As the trajectory crosses into the lower right region ($\dot{P} > 0$ and $\dot{N} > 0$) of the phase plane, both nutrient and phytoplankton levels are on the rise. Next, the trajectory crosses the N-nullcline and moves into the upper right region ($\dot{P} > 0$ and $\dot{N} < 0$) of the phase plane; phytoplankton dramatically increases while nutrients plummet as they fuel the bloom. However, at some point nutrients can no longer support further increase in P. This occurs when the trajectory passes from the upper right region into the upper left region, and crosses the P-nullcline ($\dot{P} = 0$) where the bloom attains its maximum level $P_{\max}$. Now $\dot{P} < 0$ and $\dot{N} < 0$ so that both the phytoplankton and the nutrient levels crash in the final phase (*stage*-iii) of the bloom. The phytoplankton population crashes mainly because the large nutrient pool has been depleted and the daily replacement of nutrients is not enough to support a swelling standing stock of phytoplankton.

3.2. Seasonality and skipping dynamics

We now return to our original goal of modelling recurring phytoplankton blooms by analysing the periodically forced NP model (Eq. (5)). Figs. 3–5 provide summary overviews of some of the model's different types of dynamics. The step-function forcing scheme for β (Eq. (3)) makes it possible to gain simple insights regarding the model's behaviour. We first note that each season can be associated with its own 'pseudo-equilibrium.' Here, we use the terminology 'pseudo-equilibrium' to describe the equilibrium that the model would be attracted towards if there were no changes of season. (Technically speaking the forced model has no equilibrium, stable or otherwise.) If in the case of the unforced model there is a single stable equilibrium, now the periodic forcing creates two different pseudo-equilibria between which the model jumps with every change of season. The first pseudo-equilibrium (E_L) is associated with the low season and the other (E_H) with the high season.

$$E_H = (N_H^*, P_H^*) = \left(\frac{1}{1+\delta}, I + \frac{q}{(1+\delta)}\right),$$

$$E_L = (N_L^*, P_L^*) = \left(\frac{1}{1-\delta}, I + \frac{q}{(1-\delta)}\right). \quad (7)$$

In addition to the pseudo-equilibria, each season has its associated set of nullclines. In practice, the N-nullclines ($P = \frac{I}{\beta^{\pm} N}$) changes very little from season to season (see Figs. 3h and 7) while the two vertical P-nullclines ($N = \frac{1}{\beta^{\pm}}$) stand to the left- and right-hand side of the phase plane, respectively. The equilibria E_H and E_L are located at the intersections of the NP nullclines.

Recall that in the absence of periodic forcing, the model's trajectory spirals in phase space to a single

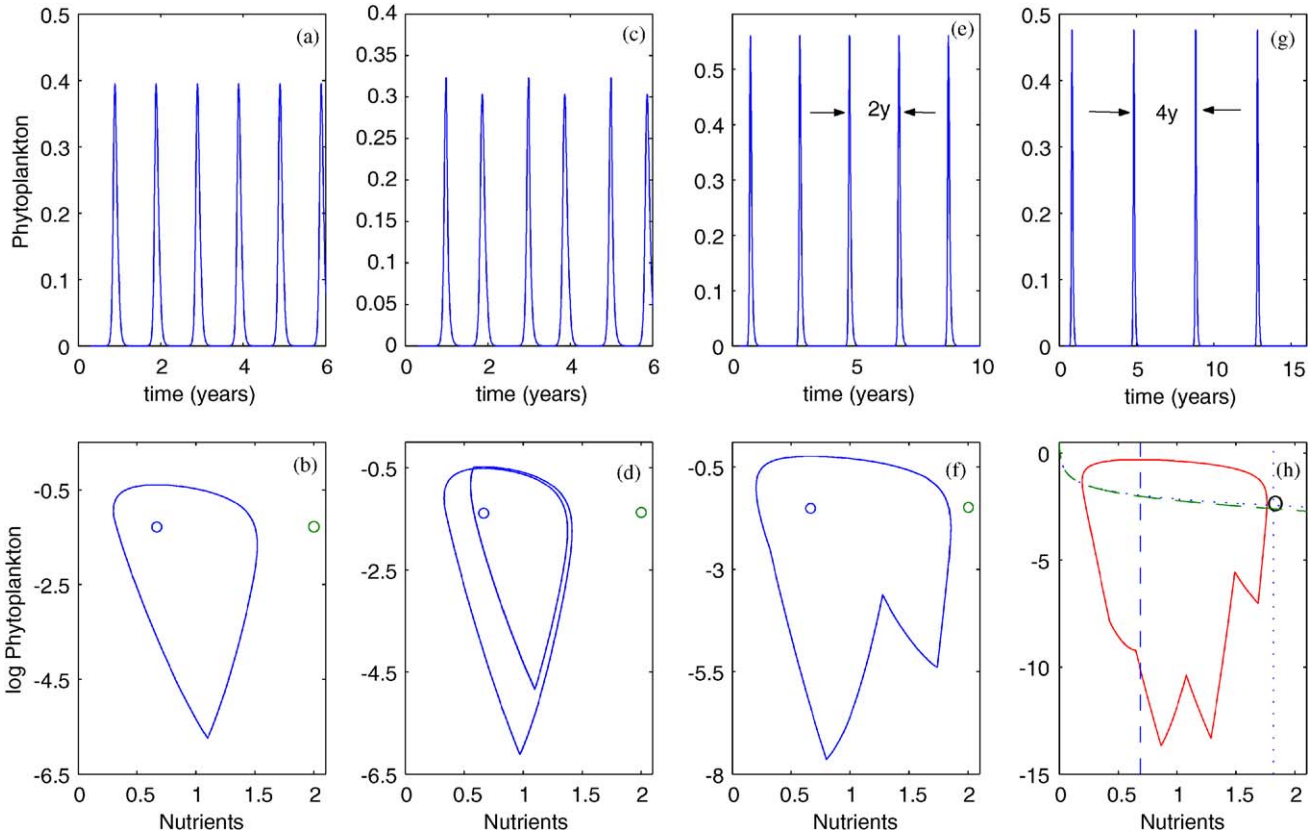

Fig. 3. Periodic solutions of seasonally forced model equations (5) for different parameters. Top panel: Time-series. Bottom panel: Phase plane (open circles represent the pseudo-equilibria which the trajectory is attracted in different seasons). Note the logarithmic scale used for the vertical axis (phytoplankton) of the phase plane where e.g. -2 refers to a population of 10^{-2}. (a,b) ($I = 0.05$) Limit cycle with annual bloom. (c,d) ($I = 0.04$) Period two cycle with bloom maxima alternating in amplitude every other year. (e,f) ($I = 0.03$) period two with skips. The main bloom occurs every second year followed by a skip (2y represents 2 years between blooms). (g,h) ($I = 0.014$) Periodic solution with a bloom every 4 years, and three skips between consecutive bloom events. The dashed lines represent the N and P nullclines associated with the high season (β^+) while the dotted line represent those associated with the low season (β^-). Parameters: $q = 0.0012,\ \omega = 0.19,\ \delta = 0.5$.

stable equilibrium as it traces out the path of the generic bloom event. However, with the inclusion of periodic forcing the trajectory is prevented from ever reaching this equilibrium. Instead, with each change of season, the direction of the trajectory is kicked away from its original path towards one 'pseudo-equilibrium' whereupon it becomes attracted to the other 'pseudo-equilibrium.' The resulting trajectory can follow a much more complicated geometry than the 'spiral to equilibrium' of the unforced system. In the simplest scenario the trajectory may form a closed loop in phase space corresponding to an annual limit cycle as seen in Fig. 3a and b. The NP phase-plane representation of Fig. 3b displays the model trajectory as it is attracted from one equilibrium to another while continually rotating in the phase plane.

We now examine exactly the same model used to generate Fig. 3a and b (with $I = 0.05$) but after reducing the inflow to $I = 0.04$. Fig. 3c shows that the dynamics are now biennial with the bloom heights alternating from 1 year to the next in the form of a two cycle. Fig. 3d displays the phase-plane representation of the biennial limit cycle.

With smaller inflow ($I = 0.03$) the model generates a qualitatively different biennial cycle (Fig. 3e). Now there is a succession of yearly blooms, but with a major bloom always followed by an extremely small bloom. In actual fact the minor bloom is too small to be identified in Fig. 3e but may be readily visualized in the phase-plane portrait of Fig. 3f where a logarithmic scale is used. The major peak is to be found in the upper part of the phase plane and is to be associated with the peak of the generic phytoplankton bloom. The minor bloom arises because the trajectory is curtailed in the phase plane and prevented from ever triggering a large amplitude bloom. We refer to this inhibition of a large amplitude bloom as a 'skip'.

To understand how skips arise, first note that at the beginning of the High season the trajectory is found in the bottom left-hand side of the phase plane and attracted to the pseudo-equilibrium E_H which it spirals towards. But this growth is interrupted when the seasons

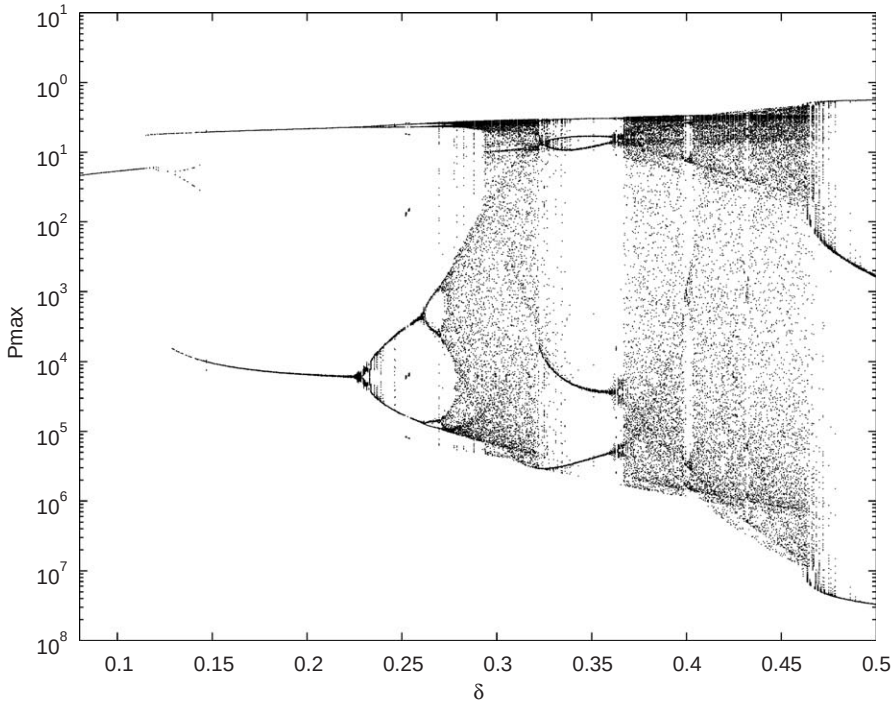

Fig. 4. Bifurcation diagram of Eq. (5). Phytoplankton maxima plotted as a function of seasonal forcing strength δ ($I = 0.02,\ q = 0.0012,\ \omega = 0.19$).

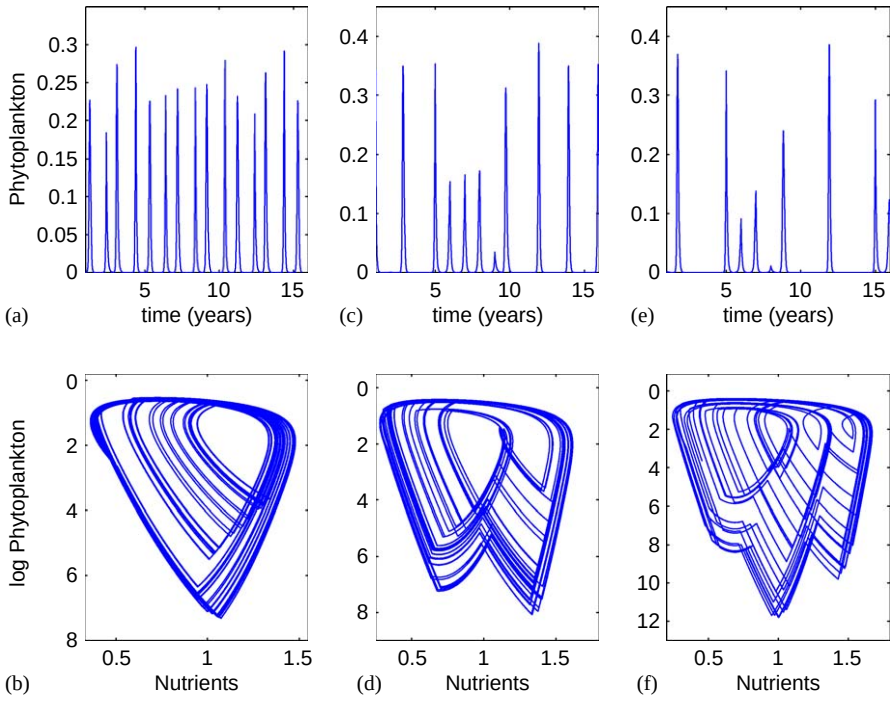

Fig. 5. Chaotic solutions of the forced model (5). Top panel: Time-series. Middle panel: Phase plane with logarithmic scale as in Fig. 3. Bottom panel: histograms of the month where the bloom maximum occurs. (a,b) Chaotic attractor with annual bloom ($I = 0.027,\ q = 0.0012,\ \omega = 0.147,\ \delta = 0.38$). (c,d) Chaotic attractor with blooms in some years and skips of 1 year in others ($I = 0.022,\ q = 0.0012,\ \omega = 0.19,\ \delta = 0.45$). (e,f) Chaotic attractor with skips of up to 2 years ($I = 0.015,\ q = 0.0012,\ \omega = 0.19$ and $\delta = 0.45$).

change. The trajectory then becomes attracted to the low season equilibrium E_L which sits on the right-hand side of the phase plane. Thus instead of the bloom continuing, the sudden change of season cuts short the growth phase, and the phytoplankton begins its decline. It is important to note that during a skip, nutrient levels

always continue to increase despite the fact that phytoplankton levels pass through a maximum. This contrasts to the pattern observed for the generic phytoplankton bloom where the nutrients increase and then decline before the phytoplankton reaches a maximum.

Skips come in many shapes and forms. In the biennial cycle of Fig. 3e–f there is a single skip every 2 years. Upon reducing inflow even further to $I = 0.014$, leads to a scenario in which there are multiple skips (Fig. 3g and h), with a bloom occurring every 4 years and there are three skips between bloom events. The phase plane shows a 'tooth-like' structure with three peaks at the transition points of each skip followed by a generic bloom event every 4 years.

In some simulations, especially when there are multiple skips, the populations range over many orders of magnitude. Real phytoplankton populations do in fact have this feature. Thus, Beltrami (1989) published data for blooms that ranged over some six orders of magnitude while the Kinneret ranges over five. Fig. 3h, however, shows that in some parameter regimes the simulations can become extreme, implying that model populations would reach unrealistically low levels. Shortly, we will describe several important and ecologically realistic modifications that eliminate this problem.

3.3. Complex behaviour

The model's different dynamics are best summarized in the bifurcation diagram of Fig. 4a where the maxima in phytoplankton numbers are plotted as a function of the forcing strength δ. For weak forcing there is a limit cycle of period 1 year as indicated by the single line in the bifurcation diagram when δ is in the range $0.09 < \delta < 0.11$. A typical limit cycle in this range would appear rather like the time-series shown in Fig. 3a or as the phase-plane portrait in Fig. 3b.

From Fig. 4a it becomes evident that as the forcing δ increases a bifurcation occurs and the limit cycle changes to period two. When $\delta = 0.155$, for example, there are now two points in the bifurcation diagram for each value of δ indicating how the peak of the annual bloom jumps between two values (High $-->$ Low $-->$ High..., etc.) each year (see also Fig. 3c–f). Increasing δ further gives rise to a complex set of bifurcations that follow the period doubling route to chaos ($0.2 < \delta < 0.315$). The chaos appears as a black band in the bifurcation diagram since for each value of δ there are now an infinite number of possible phytoplankton maxima.

The bifurcation diagram of Fig. 4 makes clear that large proportions of parameter space are dominated by chaotic behaviour. These warrant further discussion and we proceed by examining several representative time-series. Firstly, Fig. 5a shows a model simulation in which there is an annual phytoplankton bloom but the dynamics are nevertheless chaotic. The chaos manifests in two ways:

- (i) the peak heights of the phytoplankton blooms are erratic and not easily predictable.
- (ii) the time between consecutive peaks of the bloom is regular and approximately one year.

This behaviour is referred to as UPCA (uniform phase chaotic amplitude, see Blasius et al., 1999), implying that the regularity in phase growth or timing is constant but the amplitude of the bloom is chaotic.

With different parameters the models dynamics can be even more irregular as shown in Fig. 5c. Now the model time-series jumps erratically between a period-one component and period-two component. This corresponds to jumping between the 'inner' and 'outer loops' of the phase plane (Fig. 5d). On some occassions the trajectory circuits the 'outer loop,' a process that takes approximately 2 years, in which case a major bloom 1 year is followed by a skip (i.e. a minor bloom) in the next year (cf. Fig. 3f). On other occassions the trajectory circuits the smaller inner loops, which generates a set of consecutive major bloom events each year.

Fig. 5e and f show how reduction in the inflow I can induce skipping events. Thus for the same parameters that produced Fig. 5a slight reduction in I significantly suppresses bloom events and induces skips of up to two years. The skips can be seen in the lower part of the phase plane of Fig. 5f producing once again a 'tooth-like' structure.

Another model complexity arises from the existence of multiple coexisting attractors. This is shown in Fig. 6 where for a given set of parameters the model (5) may have a number of different solutions each characterized by its own unique qualitative dynamics. The solution that the model finally converges to depends on the model's initial conditions. This is further demonstrated in Fig. 6b which depicts the time-series of three such coexisting attractors, one being chaotic and the other two periodic. The existence of multiple attractors can have important ecological consequences. In real ecological systems, if there are several coexisting attractors, it may be difficult or even impossible to predict which attractor the system will eventually converge to. This will be especially true if the system's initial conditions are situated close to the edge of different basins of attraction. Multiple attractors have been noted in many other ecological models (e.g. Rinaldi et al., 1993; Earn et al., 2000; Henson, 2000; Huisman and Weissing, 2001; Vandermeer et al., 2001), and have also been verified in Daphnia-algae systems under laboratory conditions (McCauley et al., 1999).

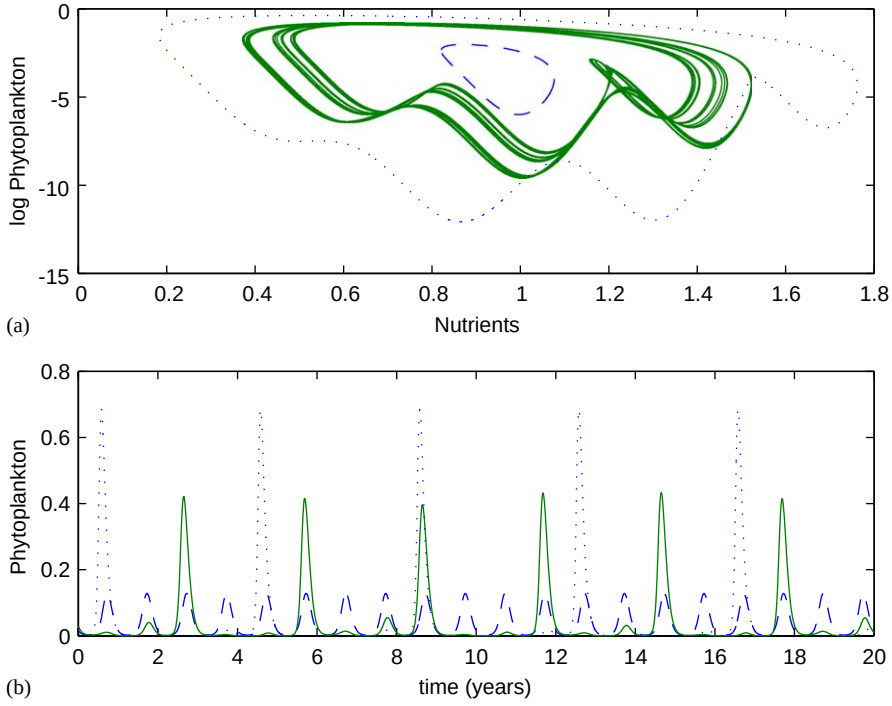

Fig. 6. Multiple coexisting attractors. (a) Phase-plane portrait of three different coexisting attractors resulting from different initial conditions. (i) Period one limit cycle—dashed line ($N_0 = 0.01$, $P_0 = 0.01$); (ii) chaotic attractor (roughly period three)—solid line ($N_0 = 0.1$, $P_0 = 0.1$); period four limit cycle—dotted line ($N_0 = 1$ and $P_0 = 1$). Parameters: $I = 0.04$, $\omega = 0.538$, $\delta = 1$ with sinusoidal forcing. (b) as in (a) plotted in the time domain.

4. Reconstructing the phase-plane dynamics

We now proceed further and attempt to gain a deeper understanding of the dynamical principals that lead to skips between bloom events. To simplify the analysis we assume that the nutrient loss rate is negligible and set $q = 0$ in Eq. (5); this has little qualitative effect on the model's dynamics when $q < \frac{I}{2}$ (see Huppert et al., 2002). It is also assumed that the nutrient influx is much smaller than phytoplankton mortality rate i.e. $I \ll 1$ for the given scaling. Under these conditions the forced NP model represents a classical slow-fast system. This can be easily seen in the phase plane in Fig. 7 where P changes many orders of magnitude compared to N. The nutrient dynamics in (5) is dominated by a difference of two terms: a small constant inflow rate, I, and a term $\beta^{\pm}NP$ which varies proportionally to the rapidly changing phytoplankton levels P. As a consequence it is possible approximate the dynamics of Eq. (5) in two different regimes:

- *Type* I: *Fast bloom dynamics where* $\beta NP \gg I$:

$$\dot{N} = -\beta^{\pm}NP,$$

$$\dot{P} = P(\beta^{\pm}N - 1). \tag{8}$$

This is the generic bloom model already discussed in which high phytoplankton levels ensure $\beta NP \gg I$. The bloom event is fast with the trajectory confined to the upper part of the phase plane (UPP). The solution of this system of equations may be approximated as (see Appendix B; Banks 1994):

$$N(t) = N_0 \exp(-\beta R(t))$$

$$P(t) = \frac{\sigma^2}{2\beta^2 N_0}\operatorname{sech}^2\left(\frac{1}{2}\sigma t - \phi\right) \tag{9}$$

$$R(t) = \varepsilon_1 + \varepsilon_2 \tanh\left[\frac{1}{2}\sigma t - \phi\right]$$

where ε_1, ε_2, σ and ϕ are constants defined in Appendix B.

- *Type* II: *Slow nutrient buildup where* $\beta NP \ll I$:

$$\dot{N} = I,$$

$$\dot{P} = \beta^{\pm}NP - P. \tag{10}$$

Nutrient levels slowly build up at the rate $\dot{N} = I$ and 'skips' may occur from year to year. The generic bloom event cannot trigger until nutrients have built up to a minimal threshold level, and the trajectory is thus confined to the lower part of the phase plane (LPP).

Eq. (10) can be integrated out (see Appendix B) to give the following explicit analytical solution:

$$N(t) = I(t - t_0) + N_0$$

$$P(N) = P_0 \exp\left(\frac{1}{I}(N - N_0)\left(\frac{\beta}{2}(N + N_0) - 1\right)\right] \tag{11}$$

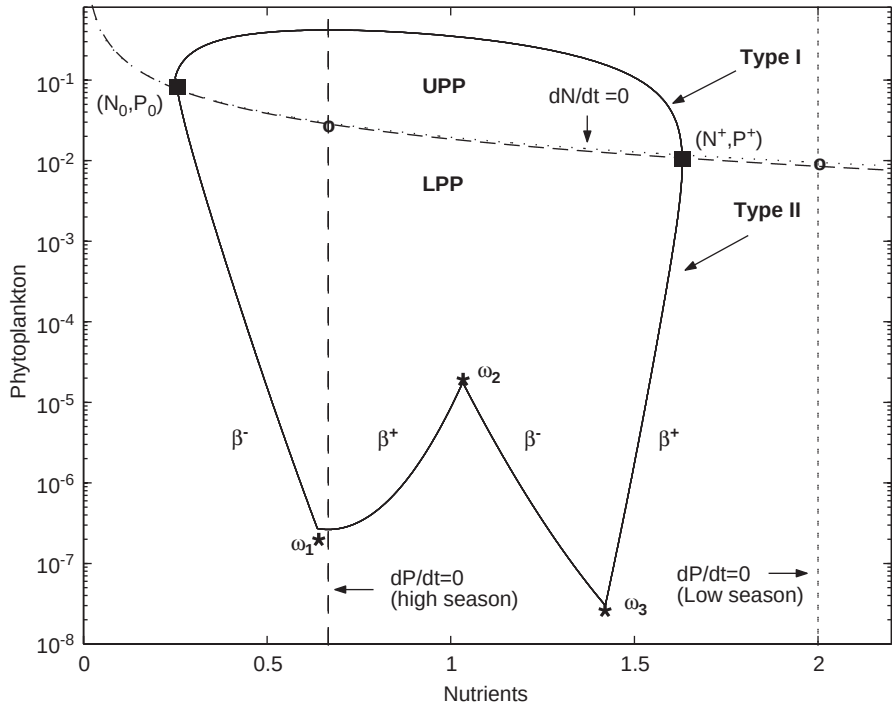

Fig. 7. Phase-plane diagram with logarithmic scale for phytoplankton. Type I solutions (the generic bloom) occur in the UPP above the N-nullcline. Type II solutions (nutrient buildup) appear in the LPP. The dashed lines represent the N- and P-nullclines associated with the high season (β^+) while the dotted line represents the N- and P-nullcline associated with the low season (β^-). Open circles represent the pseudo-equilibria. Note that the N-nullcline hardly changes between seasons, while there is a clear change in the P-nullcline. The ω_i demark the points in the phase plane when seasons change and the N-nullcline jumps from β^- to β^+ or vice-versa ($I = 0.025$, $q = 0.001$, $\omega = 0.19$ and $\delta = 0.5$).

As the forced model's trajectory spins around the phase plane it alternates between these two different types of behaviours. Thus we can use these results to formally deduce or "reconstruct" the full motion of the seasonally forced NP model in the phase plane.

At any moment, the motion of the trajectory depends both on its location in the phase plane (see Fig. 7, UPP or LPP), and on the particular timing, e.g. high (β^+) or low (β^-) season. Thus, at a certain time point the system is described by one of four possible analytic solutions i.e. they can be either Type I or Type II solutions calculated for either the High or Low season. Since Eqs. 9 and 11 gives the analytic approximations of each of these solutions, we are able to trace out the trajectory in the phase plane as in Fig. 7.

Fig. 7 gives a schematic sketch of how this works out in the simple case of a limit cycle. We start from an initial condition in the LPP which calls for using a Type II solutions. Then, after each change of season we switch to the analytic solution relevant for that season. These changes occur at the transition points ω_1, ω_2, and ω_3 shown in Fig. 7. As soon as the trajectory crosses the N-nullcline entering the UPP, the trajectory changes to a Type I solution. This solution is followed until it again crosses into the LPP. As a result the trajectory is found to rotate around the phase plane in the form of a limit cycle, here with a single 'skip' in the LPP. This is described in more detail in Appendix B.

When the parameters are such that the model dynamics is chaotic, the resulting reconstructed attractor obtained from the explicit Types I and II solutions is shown in Fig. 8a. The success of the analytical reconstruction scheme may be gauged by comparing the resulting attractor (Fig. 8a) to a simulation with closely matching parameters. (Slightly different parameters were needed to compensate for the change in the model's sensitive dynamics induced by the approximation.) shown in Fig. 8b. The latter was obtained by numerical integration of the actual equations (5) using the step-function forcing scheme. Similar good agreement can be found also in other parameter regimes for the other attractors (limit cycles of all periods as well as other chaotic attractors). Comparing Fig. 8b and c shows that the model solution is robust to the specific form of $\beta(t)$ which is chosen as step-function and sinusoidal forcing, respectively.

For other parameter regimes, this procedure can lead to more complicated dynamics (including larger number of skips, multiple attractors). In principle, by using the four different analytic solutions it is possible to describe the flow in phase space for any set of parameters. Even though in practice, this might be difficult to carry out,

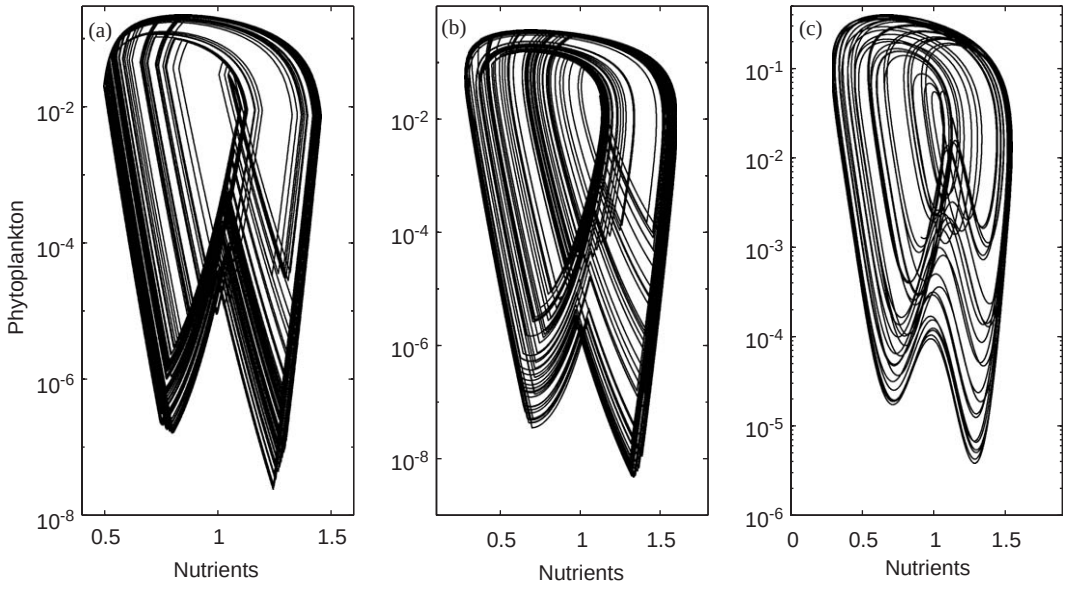

Fig. 8. (a) Reconstruction of the trajectory in the phase plane using analytic solutions obtained by Types I and II approximations (see text for details. $I = 0.015,\ \tau = 33$ and $\delta = 0.5$. (b) Simulations with Eq. (5) and β taken as a step-function (Eq. (3)) $I = 0.021,\ \tau = 33$ and $\delta = 0.5$). (c) as in (b), but with sinusoidal forcing (Eq. (2)) ($I = 0.034,\ q = 0.0012,\ \tau = 30,\ \delta = 0.6$).

we are able to grasp the essential principles governing the system dynamics. The excellent agreement between numerical solutions and the analytical results demonstrates clearly that our heuristic understanding of the model dynamics is correct.

5. More realistic models

The simple NP model studied here can be understood as a strategic model which contains only the most essential ingredients to describe bottom-up controlled seasonally recurring phytoplankton blooms. The question however remains, as to the realism of such a simplified model. In this section therefore, we introduce various additions into the model which might be regarded as essential.

5.1. Phytoplankton cysts

When modelling the dynamics of biological populations, a deterministic model is usually a sufficient approximation provided that population numbers never become too small. In the case of phytoplankton the lower bound is set by the unit of the single individual algae cell. During the course of a phytoplankton bloom, it is not uncommon for an algae population to vary in number by some six orders of magnitude or more (Beltrami, 1989). Given that the phytoplankon population in our model can easily vary many orders of magnitude, the deterministic description given by Eq. (5) should be expected to break down in cases where the variation in P exceeds seven orders of magnitude. As the phase planes of Figs. 3 and 5 indicate, such unrealistically small phytoplankton densities arise only for parameter regimes of the model for which there are multiple skips. In this case, with each skip the trajectory in the plane dives deeper and deeper downwards until finally the phytoplankton levels drop below the persistence threshold. It is reasonable to treat such an event as a local extinction. Note that the effects of demographic noise are enhanced in the vicinity of the 'extinction threshold'. Due to the low algae population levels random perturbations can easily kick the phytoplankton below threshold leading to extinction.

However, in many aquatic environments phytoplankton blooms recur even despite these skips. One plausible mechanism which enhances the persistence of algae is the formation of cysts. Cysts are a vegetative form of phytoplankton that can survive hostile environmental conditions, and are usually present in the sediment or lower water levels. The cysts can be resuspended to the photic zone by hydrodynamical processes such as upwelling or the overturn of the water column at the termination of stratification.

As a first approximation, cysts dynamics can be incorporated into the model by a small constant phytoplankton influx term, c, as follows:

$$\dot{N} = I - \beta^{\pm} NP - qN,$$

$$\dot{P} = \beta^{\pm} NP - P + c. \tag{12}$$

(Alternatively, c might be interpreted as an immigration of phytoplankton from nearby patches.)

First, consider a case without cysts ($c = 0$) and with the model parameterized in a region which yields a

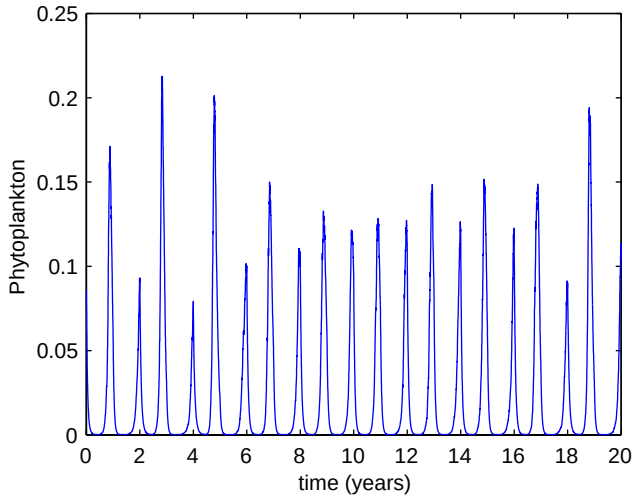

Fig. 9. Phytoplankton time-series with the combined effect of cysts and multiplicative noise (12). Parameters ($I = 0.025$, $q = 0.0012$, $\omega = 0.19$, $\delta = 0.45$, $\sigma = 0.2$, $c = 0.0001$). Note that the dynamics are UPCA.

chaotic tooth attractor similar to the one shown in Fig. 5d. With the inclusion of only a small cyst inflow rate of $c = 0.0001$, the model's natural tendency to skip disappears and is replaced by annual bloom dynamics (here an annual limit cycle). Fig. 9 is a simulation where both cysts dynamics ($c = 0.0001$) and environmental noise forcing are at work (as in Eq. (13) with $\sigma = 0.2$). In order to introduce environmental noise into our model, we modify the seasonality in (2), (3) to the form

$$\tilde{\beta}(t) = \beta(t)(1 + \eta(t)), \tag{13}$$

where $\eta(t)$ is a Gaussian white noise with mean zero and standard deviation σ. As can be seen the model's dynamics are once again annual but with erratic peaks resulting in the desired UPCA time-series.

To conclude, a small inflow of cysts effectively boosts the phytoplankton population at the minima of the cycle. Fig. 9 shows that this boost is relatively large since, skips fail to occur and annual bloom dynamics dominate. (The phytoplankton here ranges over 5 orders of magnitude.) Depending on the cysts inflow, there is a lower limit for the smallest phytoplankton densities of the model. Therefore, by inclusion of parameter c unrealistic small P-levels in the model are systematically avoided.

5.2. Monod nutrient uptake and UPCA dynamics

One of the characteristics of the basic NP model is its tendency to 'skip' and this occurs over large parameter regimes. We have found that UPCA dynamics (i.e. without skips) can be achieved by changing the functional form of the nutrient uptake terms. As is well known, under laboratory conditions the nutrient–phytoplankton interaction is more realistically described by the classical Monod equation (DeAngelis, 1992) equivalently referred to as a Holling Type II functional form. The leads to the following equations:

$$\dot{N} = I - b\beta(t)\frac{NP}{k+N} - qN,$$

$$\dot{P} = c\beta(t)\frac{NP}{k+N} - dP. \tag{14}$$

Fig. 10a presents the time-series for a typical simulation of Eq. (14) in the chaotic regime where the annual dynamics could be reasonably termed UPCA. The phase plane in Fig. 10b demonstrates that there are no skips, something which holds over a large parameter range, and that the phytoplankton population is well above the extinction threshold. Nevertheless there are parameters in which the model gives rise to skips, but in this case the phytoplankton population remains above the extinction threshold (see Fig. 10c and d). Comparison of Fig. 10d with Figs. 5 and 8 clearly show that the basic mechanism of chaos and the recurrence of phytoplankton blooms (as was developed before for the simple Lotka–Volterra uptake rate) prevails also in the case of the saturated uptake rate. The basic topology of the attractor remains unchanged, even though uptake saturation is introduced. However the attractor is deformed. The reason for this deformation is due to the modified position of the nullclines of the more realistic model equations (14). Thus, we conclude that our basic methods, which were developed here for the simple model equations (5), could be extended also to more complicated functional forms such as the Monod.

These features can be explained by the functional form of the Monod nutrient uptake which permits larger growth rates at small nutrient levels than the linear functional form under the constraint that growth rates must eventually saturate. A detailed analysis of this effect is beyond the scope of the present paper and will be described elsewhere (Olinky et al. ms). The Monod functional form thus seems to enhance UPCA dynamics in a model for which this effect is otherwise difficult to produce.

6. Conclusion

The basic NP bloom model stands in a class of other simple standard ecological outbreak models (Ludwig et al., 1978; Truscott and Brindley, 1994) which aim at understanding the processes which lead to population outbreaks. There are two fundamental differences between the earlier outbreak models to the Eq. (5) advocated here. Firstly, previous models rely on top-down effects such as predation to induce outbreaks while our model (5) is relevant for blooms that are

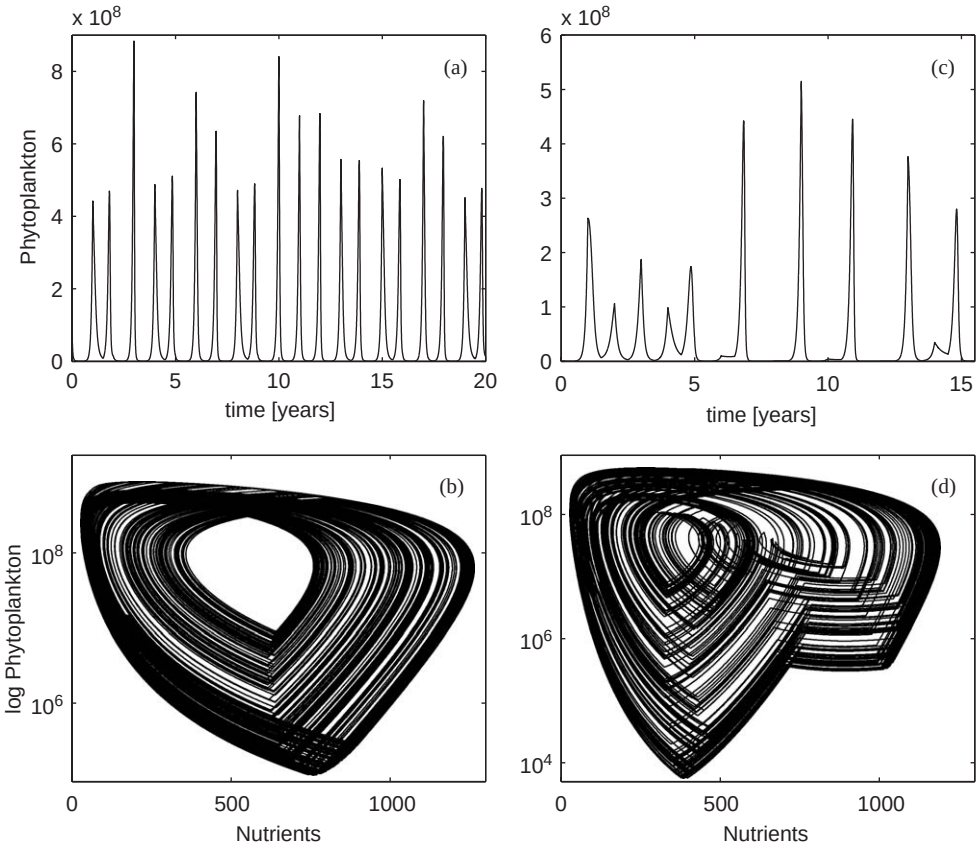

Fig. 10. UPCA dynamics generated from Eq. (14) using the Monod uptake term. Top panel: Time-series. Bottom panel: Phase plane with logarithmic scale as in Fig. 5. (a,b) Chaotic attractor with annual bloom parameters are: $I = 1500$, $b = 0.0000204$, $c = 87$, $d = 73$, $q = 0.1$, $k = 65$, $\delta = 0.12$. (c,d) Chaotic attractor with blooms in some years and skips of 1 year in others ($\delta = 0.075$, $I = 720$).

'bottom-up' or nutrient controlled. With this, however, we do not intend to suggest that bottom-up regulation is more important than top-down control, nor would we want to enter this controversial debate. Secondly, many of the previous models are based around excitable system theory. In the excitable paradigm the trajectories are confined in phase space by cubic nullclines which rigidly fix the amplitude of the bloom i.e. there is only minor variability in bloom height from one outbreak to the next. In contrast, the bloom produced by Eq. (5) is governed by spiral dynamics in the phase plane and provides a very natural and simple way to simulate irregular phytoplankton blooms.

Many phytoplankton blooms occur annually and it is a rare event if in some year a bloom fails to appear. In our attempt to model annual blooms, it was therefore somewhat surprising to find that the seasonally forced NP model (Eq. (5)) does not easily produce regular annual blooms in the chaotic parameter regime. Instead skipping events tend to occur with great frequency. To overcome this shortcoming we investigated three different scenarios. The first was the addition of demographic noise in the growth rate. Secondly we included cysts in the model which act to increase the population size. Finally we replaced the bilinear Lotka–Volterra interaction terms with a Monod saturation functional form. All three modified models successfully generated bloom dynamics with outbreaks each year having erratic amplitudes. In addition, we found that by using the Monod functional form and/or adding cysts dynamics enables phytoplankton levels in the model to remain above the extinction threshold and solve the main drawback of the simpler model. That is, the Monod-based model generates UPCA dynamics and there is a large parameter range for which populations never fall below unrealistical levels.

To conclude, the strategic NP models we have investigated might form the basis of more complex predictive management models that could be used for considering or even simulating aquatic decision making policies. The different mechanisms behind the bloom dynamics seem to be generic to the basic structure of the NP model and should therefore serve as a useful guide of scenarios to expect when incorporating greater biological realism (e.g. with multiple phytoplankton species, higher tropic levels etc.). But this work is a warning sign as well. We find that it is extremely difficult, if not impossible, to predict phytoplankton

blooms in advance given the sensitivity of the bloom to the nonlinearities of the growth process and the presence of environmental noise. These factors can easily influence the bloom's skipping dynamics and act as a fine control on the triggering of bloom events.

Acknowledgements

We thank Utza Pollingher, and Tamar Zohary for kindly allowing us to make use of field data collected at Lake Kinneret. We gratefully acknowledge support from the James S. McDonnell Foundation, and the European Union Fifth Framework grant 'Phytoplankton On-Line.' B.B. was supported by German Volkswagen Stiftung.

Appendix A

Below we show that the basic NP-model (Eq. (1) with $\beta(t)=1$), can never generate an oscillatory solution. Without loss of generality it is possible to rescale equations (1) to the simpler parameters $b=c=d$, $a=I$ & $e=q$. First using vector notation, we set $\vec{x}=[N,P]$. Dulac's criterion (Strogatz, 1994) states that if there exists a continuously differentiable real-valued function g such that $\nabla\cdot(g\frac{\mathrm{d}\vec{x}}{\mathrm{d}t})$ is of one sign only in the positive quadrant, then the model cannot have limit cycle solutions. If we set $g=\frac{1}{NP}$ then

$$\begin{aligned}\nabla\cdot\left(g\frac{\mathrm{d}\vec{x}}{\mathrm{d}t}\right)&=\frac{\partial}{\partial N}\left(g\frac{\mathrm{d}N}{\mathrm{d}t}\right)+\frac{\partial}{\partial P}\left(g\frac{\mathrm{d}P}{\mathrm{d}t}\right),\\&=\frac{\partial}{\partial N}\left(\frac{I}{NP}-1-\frac{q}{P}\right)+\frac{\partial}{\partial P}\left(1-\frac{1}{N}\right)\\&=\frac{-I}{PN^2}<0,\end{aligned}$$

which is always satisfied in the positive orthant. Hence, by Dulac's criterion, there can be no limit cycles. Using Dulac's criterion on the same model but with a Michaelis–Menten interaction term (see Eq. (14)) again rules out the possibility of limit cycle solutions.

Appendix B

Here we approximate of the motion of the trajectory in phase space for the forced model.

B.1. Type I solutions: The generic bloom

By looking at the phase plane (Fig. 7), one sees that Type I (fast bloom dynamics) solutions are initiated when the trajectory crosses the N-nullcline and enters the upper part of the phase plane (UPP). (Note that this entry point is actually the end point of Type II solutions which we specify shortly.) Let this entry point serve as the initial conditions $(N^{\dagger},P^{\dagger})$, which will be used for deriving the model trajectory in the UPP.

Eq. (8) show that the rate $(\dot{R})$ of phytoplankton removed or lost from the water column during the bloom is $\dot{R}=P$. Let us define

$$R=-\frac{1}{\beta}\ln\frac{N}{N^{\dagger}}. \tag{B.1}$$

It follows directly that $\dot{R}=-\frac{1}{\beta N}\dot{N}$ with initial condition $R^{\dagger}=0$. Banks (1994) shows how to obtain an analytic approximation of $R(t)$, $N(t)$ and $P(t)$ for a given value of β. First introduce the variables

$$\sigma^2=(\beta N^{\dagger}-1)^2+2\beta^2N^{\dagger}P^{\dagger},$$

$$\phi=\mathrm{a\ tanh}\frac{N^{\dagger}\beta-1}{\sigma},\quad \tilde{t}=\frac{1}{2}\sigma t-\phi,$$

where $\tilde{t}$ is a scaled time. Then, following Banks (1994) the dynamics of R is given by

$$R(t)=\frac{1}{\beta^2N^{\dagger}}[\beta N^{\dagger}-1+\sigma\tanh(\tilde{t})]. \tag{B.2}$$

From this we immediately deduce the time course of P

$$P(t)=\dot{R}(t)=\frac{\sigma^2}{2\beta^2N^{\dagger}}\,\mathrm{sech}^2(\tilde{t}) \tag{B.3}$$

and using (B.1), that of $N(t)$

$$N(t)=N^{\dagger}\exp(-\beta R(t)). \tag{B.4}$$

It is easy to see that $P(t)$ obtains its maximal value $P_{\max}=\frac{\sigma^2}{2\beta^2N^{\dagger}}$ at time $\tilde{t}=0$. The definition of R together with Eq. (8) is very similar to the classical SIR epidemic equations (see e.g. Murray, 1989; Banks, 1994). However, the classical scheme of the SIR outbreak does not contain a description of seasonality. While in the traditional analysis the trajectory in the phase plane could be derived by straightforward integration of $\frac{\mathrm{d}P}{\mathrm{d}N}$, in our case this scheme holds until the season changes. At this point it is necessary to continue the integration only after switching to the appropriate value of β.

Under the assumption that an outbreak event is initiated in the high season, begin by integrating equations (8) with a constant $\beta=\beta^{+}$ and the initial condition $(N^{\dagger},P^{\dagger})$. The solution is given by Eqs. (B.3) and (B.4). If the seasons change, we continue with $\beta=\beta^{-}$ and with initial conditions that are given by the final state at the change of seasons. The bloom dynamics ends at $t=t_0$ where the trajectory crosses once again the N nullcline, where $P(t_0)=\frac{I}{\beta N(t_0)}$. We are thus able to calculate the entrance point (N_0,P_0) to the Type II model, which serve as initial conditions for solving Eq. (10).

B.2. Type II: Slow nutrient buildup

We continue to approximate the model's trajectory but focus now on the flow of Type II solutions (slow nutrient buildup) in the lower part of the phase plane (LPP). Recall that a year is taken to have only two seasons. It begins in the low season at times t_k, $k = 0, 2, 4\ldots$ with a low growth rate $\beta^- = 1 - \delta$, followed by high seasons at times t_k, $k = 1, 3, 5\ldots$ with high growth rate $\beta^+ = 1 + \delta$. The length of each season is given by the constant $T = t_{n+1} - t_n$ and during this period the growth rate is constant (i.e. either β^- or β^+). Eq. (10) describing Type II solutions are studied in terms of the new variable

$$\lambda = \ln(P), \tag{B.5}$$

whereby Eq. (10) become

$$\dot{N} = I,$$

$$\dot{\lambda} = \beta^{\pm} N - 1. \tag{B.6}$$

Firstly, suppose that the trajectory has just crossed the N-nullcline $N = I/\beta P$ to enter the LPP. Let t_0 be the time of entry. Suppose also that the trajectory spends n seasons in the LPP before it crosses the N-nullcline to return to the UPP and change over to a Type I solution. In total, $nT + t^* - t_0$ represents the entire time the trajectory spends as a Type II solution.

Recall that in the LPP the trajectory moves slowly from left to right, as nutrients gradually build up at a constant rate. According to (B.6) this is given by

$$N(t) = I(t - t_0) + N_0. \tag{B.7}$$

However, every time there is a change of season, a sharp point is created in the phase plane (indicated by the points $(\omega_1, \omega_2, \omega_3, \ldots)$ in Fig. 7). At these points, the trajectory abruptly changes its direction as phytoplankton growth changes from positive to negative or vice-versa. Define 'transition points' as those points in the phase plane where the vertical component of the trajectory, (P) changes direction in the phase plane. We now proceed to calculate the transition points.

Let the kth transition point have coordinates in the phase plane $\omega_k = (N_k, \lambda_k)$. Assuming that at time t_0, $\beta(t) = \beta^-$ and the initial conditions are N_0 and $\lambda_0 = \ln(\frac{I}{\beta^- N_0})$, which defines the transition point (N_0, λ_0). By Eq. (B.7) the N_k are given by

$$N_k = IkT + N_0. \tag{B.8}$$

By integrating system (B.6) between two neighbouring transition points we obtain

$$\begin{aligned}\lambda_1 - \lambda_0 &= \beta^- \int_{t_0}^{T} N(t)\,\mathrm{d}t - T + t_0 \\ &= (1-\delta)\frac{I}{2}T^2 + T((1-\delta)c_0 - 1) - c_1 \end{aligned} \tag{B.9}$$

where $c_1 = (1-\delta)\frac{I}{2}t_0^2 + t_0((1-\delta)c_0 - 1)$, and $c_0 = N_0 - It_0$.

Or in a more general way: for every $k \geqslant 2$

$$\begin{aligned}\lambda_k - \lambda_{k-1} &= \beta^{\pm} \int_{(k-1)T}^{kT} N(t)\,\mathrm{d}t - T \\ &= (1 + (-1)^k\delta) \\ &\quad \times \left[\frac{I}{2}T^2(2k-1) + Tc_0\right] - T, \end{aligned} \tag{B.10}$$

which enables us to express λ_k in recursive form to ultimately obtain

$$\begin{aligned}\lambda_k &= \lambda_0 - c_1 + \frac{I}{2}T^2[k^2 + (-1)^k\delta] \\ &\quad + T\left[k(c_0 - 1) + \frac{(-1)^k - 1}{2}\delta c_0\right], \end{aligned} \tag{B.11}$$

where $c_1 = (1-\delta)\frac{I}{2}t_0^2 + t_0((1-\delta)c_0 - 1)$, and $c_0 = N_0 - It_0$.

We thus have an expression for all the transition points $\omega_k = (N_k, \lambda_k)$ which comprise the tooth-like structure seen in the phase plane.

Finally, in order to obtain the phytoplankton trajectory between two transition points $\omega_k = (N_k, \lambda_k)$ and $\omega_{k+1} = (N_{k+1}, \lambda_{k+1})$, Eq. (B.6) gives $\mathrm{d}\lambda/\mathrm{d}N = (\beta^{\pm}N - 1)/I$, which can be integrated to give

$$\lambda(N) = \lambda_k + \frac{1}{I}\left[(N - N_k)\left(\frac{\beta}{2}(N + N_k) - 1\right)\right]. \tag{B.12}$$

This last relationship tells us that log-transformed phytoplankton levels (λ) are a quadratic function of nutrients N between any two transition points in the LPP. Hence, it is possible to calculate the exact trajectory between any two consecutive transition points in the LPP.

References

Anderson, D.M., Kaoru, Y., White, A.W., 2000. Estimated Annual Economic Impacts form Harmful Algal Blooms (HABs) in the United States. Sea Grant Woods Hole.

Banks, R.B., 1994. Growth and Diffusion Phenomena. Springer, Berlin, Heidelberg.

Beltrami, E., 1989. A mathematical model of brown tide. Estuaries 12, 13–17.

Beltrami, E., Carroll, T.O., 1994. Modeling the role of viral disease in recurrent phytoplankton blooms. J. Math. Biol. 32, 857–863.

Blasius, B., Clodong, S., 2004. Chaos in a periodically forced chemostat with algal mortality. Proc. R. Soc. London B 271, 1617–1624.

Blasius, B., Huppert, A., Stone, L., 1999. Complex dynamics and phase synchronization in spatially extended ecological systems. Nature 399 (6734), 354–359.

Cloern, J. E., 1991. Tidal stirring and phytoplankton bloom dynamics in an estuary. J. Mar. Res. 49, 203–221.

Colwell, R.R., 1996. Global climate change and infectious disease: the cholera paradigm. Science 274, 2025–2031.

DeAngelis, D.L., 1992. Dynamics of Nutrient Cycling and Food Webs. Chapman & Hall, London.

Earn, D.J.D., Rohani, P., Bolker, B.M., Grenfell, B.T., 2000. A simple model for complex dynamical transitions in epidemics. Science 287, 667–670.

Ebenhoh, W., 1988. Coexistence of an unlimited number of algae species in a model system. Theor. Popul. Biol. 34, 130–144.

Evans, G.T., 1988. A framework for discussing seasonal succession and coexistence of phytoplankton species. Limnol. Oceanogr. 33, 1027–1036.

Franke, U., Hutter, K., Johnk, K., 1999. A physical-biological coupled model for algal dynamics in lakes. Bull. Math. Biol. 61, 239–272.

Henson, S.M., 2000. Multiple attractors and resonance in periodically forced population models. Physica D 140, 33–49.

Huisman, J., Weissing, F.J., 2001. Fundamental unpredictability in multispecies competition. The Am. Nat. 157, 489–494.

Huppert, A., Blasius, B., Stone, L., 2002. A model of phytoplankton blooms. The Am. Nat. 159, 156–171.

Huppert, A., Olinky, R., Stone, L., 2004. Bottom-up excitable models of phytoplankton blooms. Bull. Math. Biol. 66, 865–878.

Ludwig, D., Jones, D.D., Holling, C.S., 1978. Qualitative analysis of insect outbreak systems: the spruce budworm and forest. J. Anim. Ecol. 47, 315–325.

McCauley, E., Nisbet, R.M., Murdoch, W.W., de Roos, A.M., Gurney, W.S.C., 1999. Large-amplitude cycles of Daphnia and its algal prey in enriched environments. Nature 402, 653–656.

Murray, J.D., 1989. Mathematical Biology. Springer, Berlin, Heidelberg.

O'Brien, W.J., 1974. The dynamics of nutrient limitation of phytoplankton algae: a model reconsidered. Ecology 55, 135–141.

Pascual, M., 1994. Periodic-response to periodic forcing of the Droop equations for phytoplankton growth. J. Math. Biol. 32, 743–759.

Rinaldi, S., Muratori, S., Kuznetsov, Y., 1993. Multiple attractors, catastrophes and chaos in seasonal perturbed predator prey communities. Bull. Math. Biol. 55, 15–35.

Smith, H.L., 1997. The periodically forced Droop model for phytoplankton growth in a chemostat. J. Math. Biol. 35, 545–556.

Stone, L., Berman, T., 1993. Positive feedback in aquatic ecosystems: the case of microbial loop. Bull. Math. Biol 55, 919–936.

Strogatz, S.H., 1994. Nonlinear Dynamics and Chaos. Addison-Wesley Publishing Company, Reading, MA.

Truscott, J.E., Brindley, J., 1994. Ocean plankton populations as excitable media. Bull. Math. Biol. 56, 981–998.

Vandermeer, J., Stone, L., Blasius, B., 2001. Categories of chaos and fractal basin boundaries in forced predator-prey models. Chaos Solitons Fractals 12, 265–276.